Ceramics-Silikáty 67 (4), 420-426 (2023)
www.ceramics-silikaty.cz doi: 10.13168/cs.2023.0042

SYNTHESIS AND CHARACTERISATION OF Ni-DOPED ZnO THIN FILMS PREPARED BY CHEMICAL BATH DEPOSITION

#HALE YILDIZAY

KGSMYO, Department of Ceramic, Kutahya Dumlupinar University, Kutahya-43000, Turkey

#E-mail: hale.yildizay@dpu.edu.tr

Submitted August 9, 2023; accepted September 14, 2023

Keywords: Ni-doped, ZnO, Materials, Thin film, Characterisation

The experimental investigations of the optical and structural properties of Ni-doped ZnO thin films produced by chemical bath depositions were carried out. While producing ZnO, $ZnCl_2$, EDTA and NH_3 were used. In this production method, Ni doping was made for the first time. The XRD results verified the formation of the Ni doped ZnO thin films with a hexagonal wurtzite structure. The increment of the Ni doping amount allowed a decrease in the average crystallite size. It was observed that the transmittance of the films increased significantly as the amount of additive increased. It was observed that the band gap increased significantly after the additive amount passed 0.6 mM. The surface roughness was calculated from the SEM images analyses of the Ni doped ZnO films by using Image J software. It was observed that the surface roughness increased as the amount of Ni increased.

INTRODUCTION

Zinc oxide (ZnO) is a versatile material with many implementation areas. It has been used in a large range of industries, from electronics to cosmetics and even as an antimicrobial agent [1-3]. ZnO's unique properties make it ideal for use in various products and processes. Zinc oxide (ZnO) nanoparticles are of interest among II-VI semiconductor materials for nanotechnology and nanoscience due to their good electrical and optical properties such as transparency, broad band width of 3.37 [eV] and large exciton binding energy of 60 meV [4-6].

In the electronics industry, ZnO is used as an electrical insulator due to its high dielectric constant and low thermal conductivity [7]. Its ability to absorb UV radiation makes it useful for light-emitting diodes (LEDs) [8], gas sensors [9, 10], photodetectors [11], solar cells [12], thin film transistors (TFTs) [13], varistors [14, 15], photocatalysts [16] and electrochromic devices, such as smart windows or displays that can change their colour depending on the intensity of the sunlight they receive [17].

The production of ZnO can be undertaken in various ways depending on the desired application and properties. Some of the most common methods include hydrothermal synthesis [18,19], magnetron sputtering [20], sol-gel technique [21,22], chemical vapour deposition (CVD) [23], non-reactive electron beam evaporation technique [24], chemical precipitation [25], pulsed laser deposition [26], the SILAR method [27], electrochemical deposition [28-30], chemical spray pyrolysis [31–33]and chemical bath deposition[34,35].

The chemical bath deposition (CBD) method has some advantages over the other methods, making it an attractive choice for many applications. Firstly, the CBD method is much simpler and more cost-effective than the other techniques, such as physical vapour deposition or sputtering. Additionally, this process can be used to produce films with excellent optical properties due to its ability to control the film thickness and composition accurately during processing. Finally, due to its low temperature requirements compared to other methods like electrodeposition or CVD growth, the CBD technique can be used in a wide variety of substrates without damaging them in any way [36-38].

The morphology of ZnO has a significant impact on its properties, such as the surface area, surface energy, and crystal structure, which affect its performance in different applications. ZnO exists in various morphologies, including nanowires, nanorods, nanobelts, nanosheets, nanoparticles, and hierarchical structures [39-43].

Nanoparticles of zinc oxide (ZnO) doped with nickel (Ni) are a promising material for many applications. They have been used in the production of solar cells, gas sensors, and even anticorrosive coatings due to their wide band gap energy and high electrical conductivity [44-46]. Ni-doped ZnO has been used in the development of spintronics devices, which utilise the spin of electrons to store and process information [47]. It has also been explored as a photocatalyst for water splitting and hydrogen production [48].

In the literature, there is only one study on obtaining ZnO using $ZnCl_2$, ethylenediaminetetraacetic acid (EDTA) and ammonia [49]. Besides, Ni doping

has not been made before in this mentioned production method. In our study, $ZnCl_2$, EDTA, ammonia and $NiCl_2$ were used together for the first time and effects of Ni doping were investigated in detail. Many remarkable results have been obtained regarding Ni-doping, one of which was observed in the surface resistivity. The surface resistivity decreased approximately ten times with the doping. The surface roughness, which increases with the increase in the amount of Ni-doping, allows the produced materials to be used as gas sensors. In our study, it was also observed that the transmittance increased up to ten times depending on the Ni doping values. This result makes Ni-doped ZnO films attractive for use in solar cells.

EXPERIMENTAL

The CBD method was chosen for the production of ZnO on glass substrates. While producing ZnO, 65 mM of $ZnCl_2$, 16 mM of EDTA were used in 100 mL of deionised water. Also, NH_3 was added until the pH was 10.1. Nickel 0, 1, 3 and 5 % were doped in the experiments and named as Ni0, Ni1, Ni2 and Ni3, respectively. The glass bath container and glass substrates were cleaned before the experiments using a 10 % HCl acid solution and then rinsed with deionised water. The final solutions were heated up to 85 ± 2 °C, the temperatures were held and were stirred at 800 rpm. The experiments were completed in 30 minutes. The experimental conditions are summarised and given in Table 1. After the deposition, the glass surface was covered with a white precipitate. The samples were rinsed with pressurised deionised water, and then at left room temperature to dry.

The film thicknesses were calculated by using the gravimetric method. The XRD results were obtained by an X-Ray Empyrean Pan Analytical model. To calculate the transmittance and band gap, an AE LAB UV-vis device was used. The morphologic characteristics were determined by using a NANO SEM 650 SEM model device. The surface roughness of the samples was determined by using image J software. Sample photos were taken for the visual analysis.

RESULTS AND DISCUSSION

Structural analysis of the Ni-doped ZnO films

The gravimetric method was used to calculate the film thicknesses and method is given in Equation 1.

$$d = \frac{(W_2 - W_1)}{\rho A} \quad (1)$$

Where, W_1 and W_2 are the weights of the glass substrate before and after deposition, respectively. A is the area of the film deposition and ρ is the theoretical density of ZnO which is 5.6 g·cm^{-3} [50]. The film thicknesses are an average of 750 nm for all the films.

In Figure 1, the XRD patterns for all the samples are given. These patterns showed that all the films formed hexagonal grain structures. The plains (010), (002), and (011) have three dense peaks that match well with ASTM card number 98-002-6170.

Samples were then analysed using XRD to understand the reaction process of the silver and the silica. Figure 2 shows the XRD patterns of the rice husk silica and Ag/SiO_2 composites with different Molar Ag concentrations at a sintering temperature of 850 °C. The XRD pattern of the rice husk silica (Figure 2) clearly reveals the most intense peak at 2θ = 21.67° and two small peaks at 31.3° and 36.4° indicating the formation of cristobalite (PDF-39-1425).

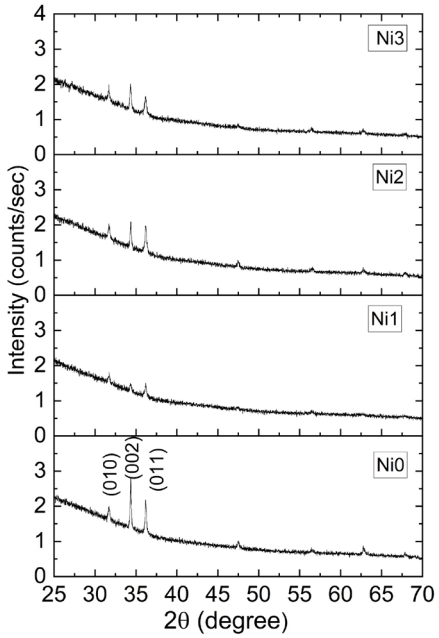

Figure 1. XRD results for the Ni-doped ZnO films.

Table 1. The summarised experimental conditions.

Experiment	$ZnCl_2$ (mM)	EDTA (mM)	pH with ammonia	$NiCl_2$ (%)	Temperature (°C)	Deposition time (min)
Ni0	65	16	10.1	0	85 ± 2	30
Ni1	65	16	10.1	1	85 ± 2	30
Ni2	65	16	10.1	3	85 ± 2	30
Ni3	65	16	10.1	5	85 ± 2	30

The crystallite sizes were calculated by using Scherrer's equation. This equation is given by Equation 2.

$$cs = \frac{0.089 * 180 * \lambda}{314 * \beta * \cos\theta_C} nm \quad (2)$$

Where λ is the wavelength of the X-Ray radiation (1.54056 Å), β is the FWHM (full width half maximum), and θ_C is the Bragg diffraction angle [51] . The crystallite sizes were calculated and are given in Table 2. As the Ni doping amount increased, the crystallite sizes decreased. The average crystallite sizes are between 41 and 34 nm.

Table 2. Crystallite sizes and band gaps.

Experiments	cs (nm) (010)	cs (nm) (002)	cs (nm) (011)	cs (nm) Average	Band gap (eV)
Ni0	36	45	39	40	3.25
Ni1	36	42	41	41	3.22
Ni2	34	41	33	36	3.80
Ni3	33	38	32	34	3.85

Optical properties of Ni-doped ZnO films

The absorbance values were obtained by UV-vis spectroscopy. The transmittance values were calculated by the absorbance values. The transmittance plots are given in Figure 2. According to Figure 2, it can be observed that the transmittance increased up to ten times depending on the Ni doping values. This result makes Ni-doped ZnO films attractive for use in solar cells.

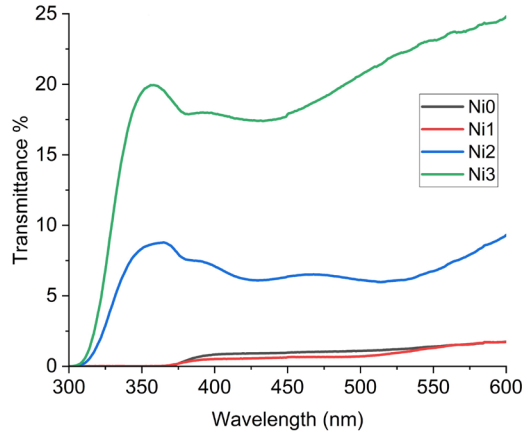

Figure 2. Transmittance plots versus wavelength.

The energy band gap values were estimated via Tauc plots, and the plots are given in Figure 3. The Tauc relation is given in Equation 3.

$$(\alpha h\upsilon) = B\left(h\upsilon - E_g\right)^n \quad (3)$$

where α is the absorption coefficient, B is a constant, hv is the photon energy, E_g is the band gap and n equals 1/2 for a direct allowed transition [33,52].

When Figure 3 is investigated, it can be seen that the band gap increases from 3.25 to 3.85 eV when the doping amount is above 3 %.

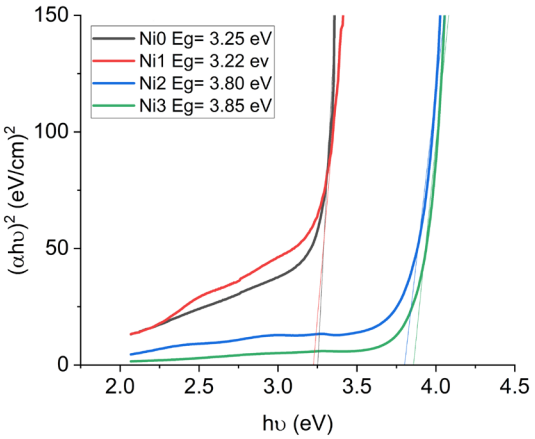

Figure 3. Tauc plots and the band gap of the Ni-doped ZnO films.

The SEM analysis of the Ni-doped ZnO films

The SEM images are given in Figure 4. The SEM images of the films were taken at 50 × magnification. There are no cracks, voids, and pinholes visible on the film surfaces.

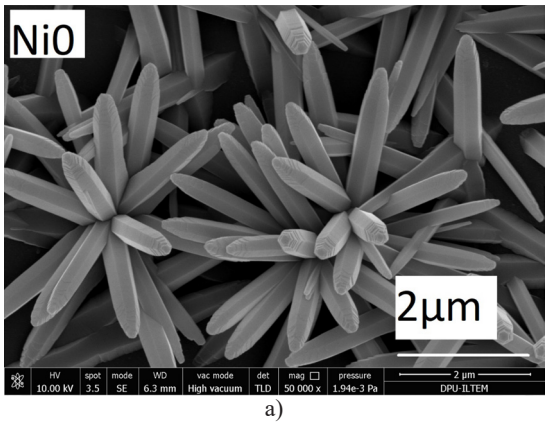

a)

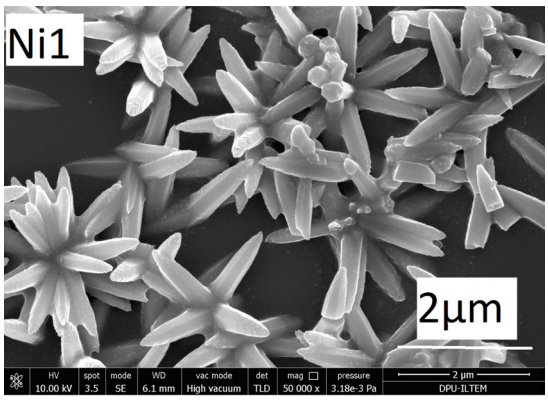

b)

continued

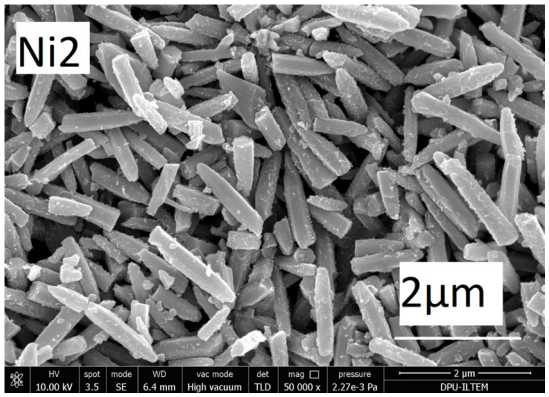

c)

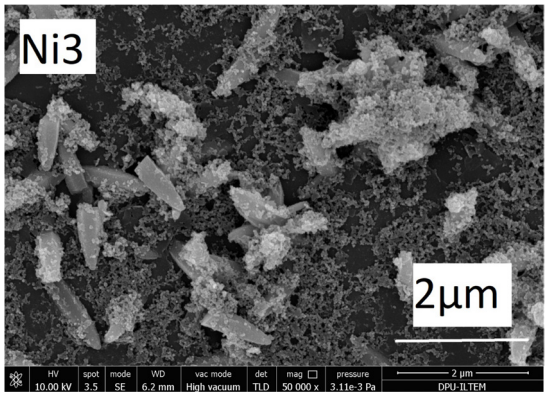

d)

Figure 4. The SEM images of the samples of the Ni-doped ZnO films.

The mean length and width of the films are given in Table 3. When Table 3 is analysed, the sizes of the nanorods decreased depending on the doping amounts.

Table 3. The sizes of the nanorods.

Samples	Mean crystallite length (nm)	Mean crystallite width (nm)
Ni0	2000	400
Ni1	1750	300
Ni2	1500	250
Ni3	1000	210

The ImageJ software was employed to calculate the surface roughness and the images are shown in Figure 5. The roughness of the films is given in Table 4.

Table 4. Values of the surface roughness calculated with ImageJ software.

Experiments	Ni doping rate	Ra (nm)	Rq (nm)
Ni0	0 %	47	42
Ni1	1 %	48	40
Ni2	3 %	57	47
Ni3	5 %	60	51

As the doping ratio increased, the roughness of the films also increased. As the roughness increases, the surface area of the samples increases. The increased surface area makes this film suitable for gas sensors.

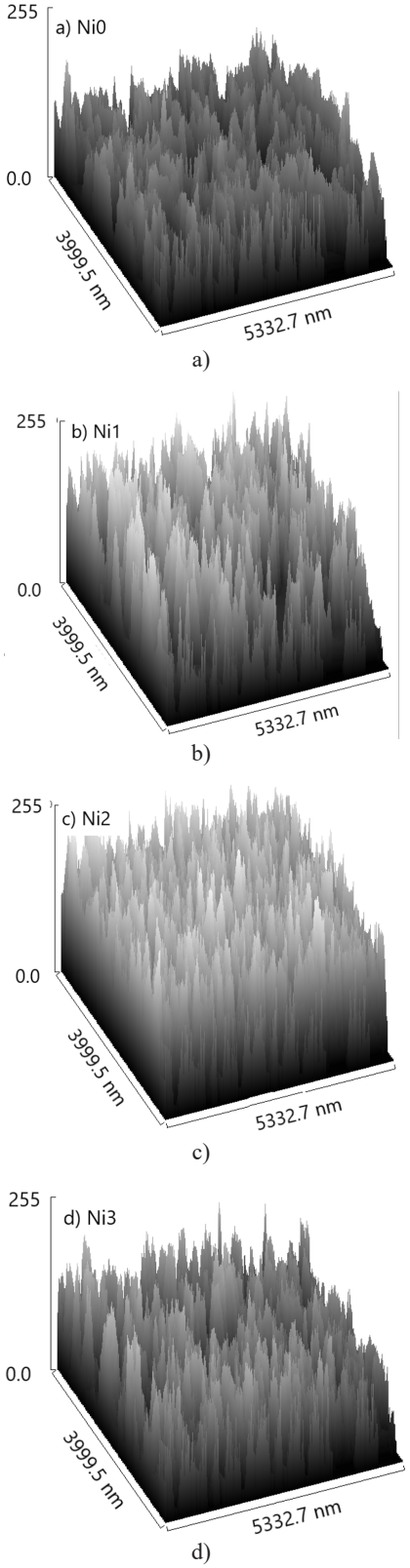

Figure 5. The surface roughness of the Ni-doped ZnO films.

Surface resistivity of Ni-doped ZnO films

The electrical properties of the films were characterised using a surface resistivity meter. This method characterises the electrical properties of thin films for conductive and semi-conductive materials. For this method, the four-probe method was used. The surface resistivity of the samples is given in Figure 6. According to Figure 6, when Ni was not used, the surface resistivity was measured as 2.1659 kΩmm. On the other hand, when the Ni was doped in the ZnO films, the surface resistivity values decreased nearly ten times.

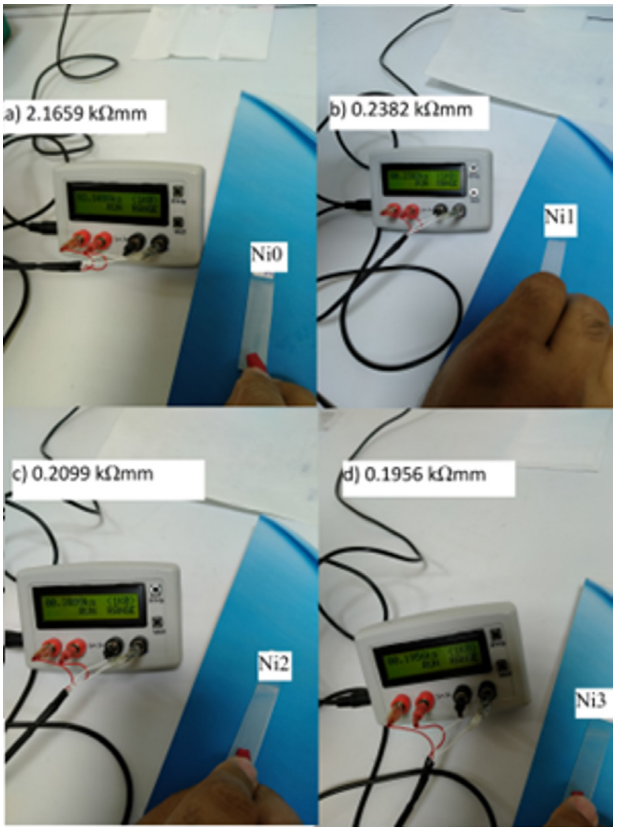

Figure 6. The surface resistivity measurement of the samples of the Ni-doped ZnO films.

Visual analysis of the Ni-doped ZnO films

For the visual analysis, a photograph of the samples was taken and is shown in Figure 7. According to the photograph, it can be seen that all the films well adhered onto glass substrates. All the films have milky colours. There are no voids, pinholes, or cracks on the surface of the films.

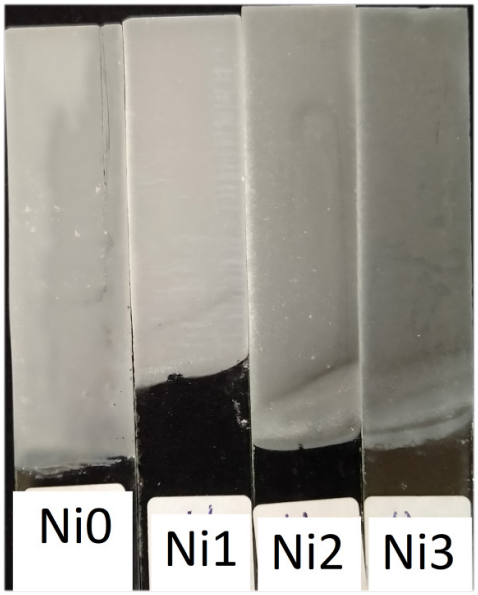

Figure 7. The photograph of the samples of the Ni-doped ZnO films.

CONCLUSIONS

In this study, ZnO films were produced, and the effects of Ni doping were investigated. Transparent semi-conductive thin films were produced with success by the chemical bath deposition technique using only $ZnCl_2$, EDTA and ammonia on the glass substrates. The films produced with these three materials were doped with Ni for the first time. The films formed in a hexagonal structure. The crystallite sizes varied from 41 to 34 nm. The optical properties were analysed using absorbance measurements. The band gap was obtained from the Tauc plot and the band gap increased significantly with the Ni doping to the films. Moreover, the band gap increased from 3.25 to 3.85 eV. The surface roughness of the films was calculated by the ImageJ software from the SEM images. It was observed that as the amount of doping increased, the surface roughness increased. The surface resistivities were measured by the four-probe method. It was observed that the surface resistivity was significantly reduced by the Ni doping. The surface resistivity decreased from 2.1659 up to 0.1956 kΩmm with the Ni doping. From the photographs of the samples, it was seen that ZnO adhered well to the surface, and no voids and cracks were formed. We believe that Ni-doped ZnO films could be used as light-emitting devices in nano-scale optoelectronic applications.

REFERENCES

1. Godlewski M., Guziewicz E., Kopalko K., Łuka G., Łukasiewicz M. I., Krajewski,T., Gierałtowska S. (2011):

Zinc oxide for electronic, photovoltaic, and optoelectronic applications. *Low Temperature Physics, 37*(3), 235–240. doi:10.1063/1.3570930
2. Spoiala A., Albu G. M., Ficai A., Andronescu E., Voicu G., Ungureanu C. (2014): The SiO2/ZnO composite materials for cosmetic creams. *Digest Journal of Nanomaterials and Biostructures, 9*(4), 1729-1737.
3. Padmavathy N., Vijayaraghavan R. (2008): Enhanced bioactivity of ZnO nanoparticles - An antimicrobial study. *Science and Technology of Advanced Materials, 9*(3), 035004 . doi:10.1088/1468-6996/9/3/035004
4. Samanta A., Goswami M. N., Mahapatra P. K. (2018): Magnetic and electric properties of Ni-doped ZnO nanoparticles exhibit diluted magnetic semiconductor in nature. *Journal of Alloys and Compounds, 730*, 399–407. doi:10.1016/j.jallcom.2017.09.334
5. Kerli S., Alver U., Tanriverdi A., Avar B. (2015): Structural and physical properties of boron doped ZnO films prepared by chemical spray pyrolysis method. *Crystallography Reports, 60*(6), 946–950. doi:10.1134/S1063774515060139
6. Baneto M., Lare Y., Cattin L., Addou M., Jondo K., Morsli M., Bernede J. C. (2010): Comparison of the Structural and Morphological Properties of Sn Doped ZnO Films Deposited by Spray Pyrolysis and Chemical Bath Deposition. *Asian Journal of Materials Science, 2*(4), 196–203. doi:10.3923/ajmskr.2010.196.203
7. Abdel–Baset T. A., Belhaj M. (2021): Structural characterization, dielectric properties, and electrical conductivity of ZnO nanoparticles synthesized by co-precipitation route. *Physica B: Condensed Matter, 616*, 413130. doi:10.1016/j.physb.2021.413130
8. Choi Y. S., Kang J. W., Hwang D. K., Park S. J. (2010): Recent advances in ZnO-based light-emitting diodes. *IEEE Transactions on Electron Devices, 57*(1), 26–41. doi:10.1109/TED.2009.2033769
9. Kang Y., Yu F., Zhang L., Wang W., Chen L., Li Y. (2021): Review of ZnO-based nanomaterials in gas sensors. *Solid State Ionics, 360*. doi:10.1016/j.ssi.2020.115544
10. Güntürkün K., Toplan Ö. (2006): Densification and grain growth of SrO-doped ZnO. *Ceramics-Silikáty, 50*, 225-231.
11. Mousavi S. S., Sajad B. (2022): Self-powered Vs. high speed ZnO-based photodetectors. *Materials Research Bulletin, 155*, 111950. doi:10.1016/j.materresbull.2022.111950
12. Wibowo A., Marsudi M. A., Amal M. I., Ananda M. B., Stephanie R., Ardy H., Diguna L. J. (2020): ZnO nanostructured materials for emerging solar cell applications. *RSC advances, 10*(70), 42838-42859. doi:10.1039/d0ra07689a
13. Jiang L., Li J., Huang K., Li S., Wang Q., Sun Z., Wang X. (2017): Low-Temperature and Solution-Processable Zinc Oxide Transistors for Transparent Electronics. *ACS Omega, 2*(12), 8990–8996. doi:10.1021/acsomega.7b01420
14. Lin J., Li S., He J., Zhang L., Liu W., Li J. (2017): Zinc interstitial as a universal microscopic origin for the electrical degradation of ZnO-based varistors under the combined DC and temperature condition. *Journal of the European Ceramic Society, 37*(11), 3535–3540. doi:10.1016/j.jeurceramsoc.2017.04.039
15. Ke L., Yuan Y., Zhao H., Ma X. (2013): Influence of rare-earth doping on the electrical properties of high voltage gradient ZnO varistors. *Ceramics-Silikaty, 57*(1), 53-57.
16. Kasumov A. M., Korotkov K. A., Karavaev, V. M., Zahorny, M. M., Dmitrie, A. I., Ievtushenk, A. I. (2021): Photocatalysis with the Use of ZnO Nanostructures as a Method for the Purification of Aquatic Environments from Dyes. *Journal of Water Chemistry and Technology, 43*(4), 281–288. doi:10.3103/s1063455x21040044
17. Chun Y. T., Neeves M., Smithwick Q., Placido F., Chu D. (2014): High optical and switching performance electrochromic devices based on a zinc oxide nanowire with poly (methyl methacrylate) gel electrolytes. *Applied Physics Letters, 105*(19). doi:10.1063/1.4901443
18. Edalati K., Shakiba A., Vahdati-Khaki J., Zebarjad S. M. (2016): Low-temperature hydrothermal synthesis of ZnO nanorods: Effects of zinc salt concentration, various solvents, and alkaline mineralizers. *Materials Research Bulletin, 74*, 374–379. doi:10.1016/j.materresbull.2015.11.001
19. Strachowski T., Baran M., Małek M., Kosturek R., Grzanka E., Mizeracki J., Marynowicz S. (2022): Hydrothermal Synthesis of Zinc Oxide Nanoparticles Using Different Chemical Reaction Stimulation Methods and Their Influence on Process Kinetics. *Materials, 15*(21). doi:10.3390/ma15217661
20. Ondo-Ndong R., Ferblantier G., Al Kalfioui M., Boyer A., Foucaran A. (2003): Properties of RF magnetron sputtered zinc oxide thin films. *Journal of Crystal Growth, 255*(1–2), 130–135. doi:10.1016/S0022-0248(03)01243-0
21. Ayachi M., Ayad F., Djelloul A., Benharrat L., Anas S. (2021): Synthesis and Characterization of Ni-Doped ZnO Thin Films Prepared by Sol–Gel Spin-Coating Method. *Semiconductors, 55*(5), 482–490. doi:10.1134/S1063782621050043
22. Patel M., Mishra S., Verma R., Shikha D. (2022): Synthesis of ZnO and CuO nanoparticles via Sol gel method and its characterization by using various technique. *Discover Materials, 2*(1),1. doi:10.1007/s43939-022-00022-6
23. Chen Z., Shum K., Salagaj T., Zhang W., Strobl K. (2010): ZnO thin films synthesized by chemical vapor deposition. In *2010 Long Island Systems, Applications and Technology Conference, LISAT 10*. doi:10.1109/LISAT.2010.5478331
24. Golshahi S., Rozati S. M., Ghasempoor T. (2011): Annealing treatment of ZnO thin films prepared by non-reactive E-beam evaporation technique. *Digest Journal of Nanomaterials and Biostructures, 6*(2), 445-450.
25. Shivaraj B., Prabhakara M. C., Bhojya Naik H. S., Indrajith Naik E., Viswanath R., Shashank M., Kumara Swamy B. E. (2021): Optical, bio-sensing, and antibacterial studies on Ni-doped ZnO nanorods, fabricated by chemical co-precipitation method. *Inorganic Chemistry Communications, 134*. doi:10.1016/j.inoche.2021.109049
26. Tsoutsouva M. G., Panagopoulos C. N., Papadimitriou D., Fasaki I., Kompitsas M. (2011): ZnO thin films prepared by pulsed laser deposition. *Materials Science and Engineering B: Solid-State Materials for Advanced Technology, 176*(6), 480–483. doi:10.1016/j.mseb.2010.03.059
27. Soltabayev B., Er İ. K., Yıldırım M. A., Aytunç A., Selim A. (2021): The Dependence of The Nickel Concentration of ZnO Thin Films for Gas Sensors Applications. *Gazi University Journal of Science Part A: Engineering and Innovation, 8*(1), 157-165. Retrieved from http://dergipark.gov.tr/gujsa.
28. Dai S., Li Y., Du Z., Carter K. R. (2013): Electrochemical Deposition of ZnO Hierarchical Nanostructures from Hydrogel Coated Electrodes. *Journal of The Electrochemical Society, 160*(4), D156–D162. doi:10.1149/2.064304jes
29. Sanchez S., Lévy-Clément C., Ivanova V. (2012):

Electrochemical Deposition of ZnO Thin Films and Nanowires for Photovoltaic Applications. Journal of *The Electrochemical Society, 159*(12), D705–D712. doi:10.1149/2.024212jes

30. Saraç U., Baykul M. C. (2021): The influence of seed layer electroplating time on structural properties, optical energy bandgap, diameter, growth orientation and surface roughness of ZnO nanorods. *Journal of Materials Science: Materials in Electronics, 32*(22), 26578–26587. doi:10.1007/s10854-021-07034-7
31. Nádherný L., Sofer, Z., Sedmidubský, D., Jankovský, O., Mikulics, M. (2012): ZnO thin films prepared by spray-pyrolysis technique from organo-metallic precursor. *Ceramics-Silikáty, 56*(2), 117-121.
32. Owoeye V. A., Ajenifuja E., Adeoye E. A., Osinkolu G. A., Popoola A. P. (2019): Microstructural and optical properties of Ni-doped ZnO thin films prepared by chemical spray pyrolysis technique. *Materials Research Express, 6*(8). doi:.1088/2053-1591/ab26d9
33. Ali M. Y., Khan M. K. R., Karim A. M. M. T., Rahman M. M., Kamruzzaman M. (2020): Effect of Ni doping on structure, morphology, and opto-transport properties of spray pyrolised ZnO nanofiber. *Heliyon, 6*(3). doi:10.1016/j.heliyon.2020.e03588
34. Önal M., Altıokka B. (2020): Effect of stirring on chemically deposited ZnO thin films. *Acta Physica Polonica A, 137*(6), 1209–1213. doi:10.12693/APhysPolA.137.1209
35. Al-Wardy R. A., Abbas A. S., Abbas S. I. (2021): Optical Properties of ZnO Films Prepared by CBD technique. *Journal of Ovonic Research, 17*(1), 53-60.
36. Önal M., Altıokka B. (2020): Pinhole-free PbS thin film production using a low-temperature chemical bath deposition method. *Journal of Nano Research, 63*, 1–9. doi:10.4028/www.scientific.net/JNanoR.63.1
37. Abbas K., Aamir M., Mehmood R. F., Sher M., Akhtar J. (2021): Deposition of morphology-Tailored CdS thin films by chemical bath approach. In Materials Today: Proceedings (Vol. 53, pp. 339–344). Elsevier Ltd. doi:10.1016/j.matpr.2022.01.365
38. Schwartz R. W., Schneller T., Waser R. (2004): Chemical solution deposition of electronic oxide films. *Comptes Rendus Chimie, 7*(5), 433–461. doi:10.1016/j.crci.2004.01.007
39. Cui J. (2012): Zinc oxide nanowires. *Materials Characterization.* Elsevier Inc. doi:10.1016/j.matchar.2011.11.017
40. Wahid K. A., Lee W. Y., Lee H. W., Teh A. S., Bien D. C. S., Azid I. A. (2013): Effect of seed annealing temperature and growth duration on hydrothermal ZnO nanorod structures and their electrical characteristics. *Applied Surface Science, 283*, 629–635. doi:10.1016/j.apsusc.2013.06.159
41. Xing G. Z., Fang X. S., Zhang Z., Wang D. D., Huang X., Guo J., Wu T. (2010): Ultrathin single-crystal ZnO nanobelts: Ag-catalyzed growth and field emission property. *Nanotechnology, 21*(25), 255701. doi:10.1088/0957-4484/21/25/255701
42. Iqbal T., Khan M. A., Mahmood H. (2018): Facile synthesis of ZnO nanosheets: Structural, antibacterial, and photocatalytic studies. *Materials Letters, 224*, 59–63. doi:10.1016/j.matlet.2018.04.078
43. Naseer M., Aslam U., Khalid B., Chen B. (2020): Green route to synthesize Zinc Oxide Nanoparticles using leaf extracts of Cassia fistula and Melia azadarach and their antibacterial potential. *Scientific Reports, 10*(1), 9055. doi:10.1038/s41598-020-65949-3
44. Mustafa S. M., Barzinjy A. A., Hamad A. H., Hamad S. M. (2022): Green synthesis of Ni doped ZnO nanoparticles using dandelion leaf extract and its solar cell applications. *Ceramics International, 48*(19), 29257–29266. doi:10.1016/j.ceramint.2022.05.202
45. Xu M., Li Q., Ma Y., Fan H. (2014): Ni-doped ZnO nanorods gas sensor: Enhanced gas-sensing properties, AC and DC electrical behaviors. Sensors and Actuators, B: Chemical, 199, 403–409. doi:10.1016/j.snb.2014.03.108
46. Ibrahim M., Kannan K., Parangusan H., Eldeib S., Shehata O., Ismail M., Sadasivuni K. K. (2020): Enhanced corrosion protection of Epoxy/ZnO-NiO nanocomposite coatings on steel. *Coatings, 10*(8), 783. doi:10.3390/COATINGS10080783
47. Mohapatra J., Mishra D. K., Kamilla S. K., Medicherla V. R. R., Phase D. M., Berma V., Singh S. K. (2011): Ni-doped ZnO: Studies on structural and magnetic properties. *Physica Status Solidi (B) Basic Research, 248*(6), 1352–1359. doi:10.1002/pssb.201046513
48. Yang T. C., Chang F. C., Wang H. P., Wei Y. L., Jou C. J. (2014): Photocatalytic splitting of seawater effected by (Ni-ZnO) @C nanoreactors. *Marine Pollution Bulletin, 85*(2), 696–699. doi:10.1016/j.marpolbul.2014.02.011
49. Önal M., Altıokka B. (2020). Optimization of EDTA–Ammonia Ratio for Chemically Deposited Layers of ZnO Nanoparticles. *Crystallography Reports, 65*(7), 1237–1241. doi:10.1134/S1063774520070135
50. Mondal S., Bhattacharyya S. R., Mitra P. (2013): Preparation of manganese-doped ZnO thin films and their characterization. *Bulletin of Materials Science, 36*, 223-229. doi:10.1007/s12034-013-0462-3
51. Bhowmik R., Murty M. N., Srinadhu E. S. (2008): Magnetic modulation in mechanical alloyed $Cr_{1.4}Fe_{0.6}O_3$ oxide. *PMC Physics B, 1*(1), 1-18. doi:10.1186/1754-0429-1-20
52. Bal I., Baykul M. C., Saraç U. (2021): The Effect of Solution Temperature on Chemically Manufactured CdS Samples. *Chalcogenide Letters, 18*, 1-10.